Communication in Physical Sciences, 2024, 11(4): 589-606

Crystal Structure, in Silico Studies and Anti-diabetic Potentials of 3-e-(1,5-dimethyl-3-oxo-2-phenyl-2,3-dihydro-1*h*-pyrazol-4-yl)hyd -razinylidene]pentane-2,4-dione(hdpp)and its Cu(II) and Ni(II) complexes

Ndidiamaka. Justina Agbo, Pius Onyeoziri Ukoha, Uchechukwu Susan Oruma*, Oguejiofo T. Ujam, Tania Groutso, Okereke Solomon Ejike
Received: 02 April 2024/Accepted: 06 July 2024/Published: 23 July 2024

Abstract: *The hydrazone, 3-E-[2-(1,5-Dimethyl-3-oxo-2-Phenyl-2,3-Dihydro-1h-Pyrazol-4-yl)Hydrazinylidene]Pentane-2,4-dione, HDPP was synthesized by coupling diazotized 4-aminoantipyrine with pentan-2,4-dione at < 5 ^{0}C. The Cu(II) and Ni(II) complexes were prepared by refluxing stoichiometric amounts of metal salts and HDPP in ethanol for 6 h at 60 ^{0}C. The ligand and complexes were characterized by UV-Vis, IR, NMR, and mass spectroscopies as well as by C, H, N, S elemental analysis, conductivity measurement, quantitative chloride determination and single crystal X-ray diffraction analysis. The compounds were screened in vitro for antibacterial activity against P. aeruginosa, S. aureus, Ecoli(Eco 6), E. coli(13), B. subtilis, S. pneumonia, P. mirabilis, S. intermedius and K. pneumoniae. The compounds were assayed for in silico molecular docking and in vivo anti-diabetic potentials. FTIR data showed shifts in ν(C=O), ν(N=H) and ν(C=N) of the complexes implicating the involvement of these groups in complexation. Proton NMR shifts accounted for the methyl, phenyl and N-H protons of the ligand but indecipherable for the complexes due to paramagnetic effects. Conductivity values of HDPP and complexes showed the ligand and its complexes to be neutral. X-ray crystallographic data of HDPP show the ligand to have orthorhombic crystals with pbca unit cell a = 28.501(4) Å, α = 90°, b = 15.0494(19) Å, β = 90°; and c = 7.3234(9) Å, γ = 90° with Z=8. HDPP and its complexes exist in hydrazo form instead of azo form. It showed no activity against test organisms, but the complexes showed various degrees of sensitivities against the test bacterial strain at 10μg/cm^3. Acute toxicity (LD_{50}) tests showed that HDPP and $[Cu(HDPP)_2Cl_2]$ were non-toxic. In silico studies proved them to be drug candidates for diabetes with good oral bioavailability. In vivo, antidiabetic tests showed HDPP and $[Cu(HDPP)_2Cl_2]$ to reduce the blood level of diabetic rats to within 61 to 67% better than the control drug glibenclamide within 14 days of treatment.*

Keywords: *Hydrazone, X- ray crystallography, Co(II), Ni(II), Cu(II) and Fe(III) complexes, In silico and antidiabetic studies.*

Ndidiamaka Justina Agbo
Sheda Science and Technology Complex, Abuja, Nigeria
Email: agbo.ndj@gmail.com
Orcid id: 0009-0002-0586-6375

Pius Oziri Ukoha
Coordination Chemistry and Inorganic Pharmaceuticals Unit,Department of Pure and Industrial Chemistry,University of Nigeria, Nsukka, 410001, Nigeria.
Email: pius.ukoha@unn.edu.ng
Orcid id: 0000-0003-3041-0919

***Uchechukwu Susan Oruma**
Coordination Chemistry and Inorganic Pharmaceuticals Unit,Department of Pure and Industrial Chemistry,University of Nigeria, Nsukka, 410001, Nigeria.
Email: susan.oruma@unn.edu.ng
Orcid id: 0000-0002-9226-2512

Oguejiofo Theophilus Ujam
Department of Pure and Industrial Chemistry,University of Nigeria, Nsukka, 410001, Nigeria.
Email: oguejiofo.ujam@unn.edu.ng
Orcid id: 0000-0002-5628-209x

Tania Groutso
School of Chemical Sciences, University of Auckland, Private Bag 92019, Auckland1142 New Zealand.
Email: taniagroutso@auckland.ac.nz

Solomon Ejike Okereke
Department of Industrial Chemistry, Abia State University, Uturu, Abia State
Email: solomonokereke53@gmail.com
Orcid id: 0009-0008-9037-6381

1.0 Introduction

Very scanty reports exist as regards hydrazones of β-diketones (Ravindran, 2004; Mohahan*et al.*, 2009; Budesinsky and Svecova, 1970; Morgan and Reilly, 1913). An earlier report (Ravindran, 2004; Mohahan*et al.*, 2009) showed the synthesis of hydrazone derived from 4-aminoantipyrine and penta-2,4-dione and its Fe(III) and some lanthanoid(III) nitrate complexes. However, the compounds were not fully characterized and no crystal structure reported. In their report Budesinsky and Svecova, (1970), obtained an azo compound from the reaction of pentan-2,4-dione and 4-amionantipyrine and showed the potentials of the azo compound as an analytical reagents. Much earlier Morgan and Reilly(1913) had reported the formation of the same azo compound from the same reaction. Similar compounds were obtained from the reaction of acetoacetanlide and ethylacetoacetate with diazotized 4-aminoantipyrine (Sarwar *et al.*, 2010). Only infrared and nmr data of the compounds were reported and the correct structures were not fully reported.
Hydrazones have proved to be versatile candidates in complex formation(Rao *et al*, 1997; Sivasankar and Gavindaragam,, 1995; Issa*et al*, 2001), pharmacology (Sari *et al.*, 2008; Zdzislaw, 2009; Ozmen and Olgun, 2008) and agrochemicals (Nawar and Hosny, 2000; Ghaib *et al*., 2000). They show diverse biological activities such as anticonvulsant, antidepressant, analgesic, anti-inflammatory, antiplatelet, antimalarial, antimicrobial, antimycobacterial, antitumoral, vasodilator, antiviral, schistosomiasis (Rollas and Küçükgüzel, 2007). However, there is no existing report on their usage as antidiabetic drugs.
Diabetes is a diseased condition affecting more than 9.3 % of the world's population (Blonde, 2005). Its management and treatment have proved very difficult in healthcare (Blonde, 2005). This is more so aggravated by the resistance of diabetes mellitus to insulin and existing antidiabetic drugs. Existing antidiabetic drugs on the loap men have shown high levels of toxicity with usage (Blonde, 2005). The research for more potent and less toxic antidiabetic drugs is the challenge facing chemists, and pharmacists the world over. In line with the need to derive a promising antidiabetic drug, HDPP and its Cu(II) and Ni(II) complexes were synthesized and their potentials determined.

2.0 Materials and methods

2.1 Materials and measurements

Pentan-2,4-dione, 4-aminoantipyrine, Iron(III)chloride-hexahydrate, cobalt(II)chloride, copper(II) and nickel(II)choride were purchased from Zayo-Sigms and were used as purchase without further purification. UV-Visibble data were obtained on Cecil UV-Visible spectrophotometer. FTIR data of the compounds were performed using KBr discs on a Perkin-Elmer FTIR spectrometer, NMR data on Bruker AVIII-400 NMR spectrometer whereas microanalytical data were run on Heraeus Carlo Erba 1108-CHN analyser. X-ray crystallography data of HDPP was run on a goniometer of Kappa geometry and CCD diffractometer equipped with Mo, Kα source. HDPP was corrected for absorption and polarization effects and

analysed for space group determination.

The microorganisms *P.aeruginosa B.subtilis, S.aureus,E.coli(Eco* 6), *E.coli*(*Eco*.13), *S.pneumoniae, S. intermedius* were clinical isolates fromhuman, while *P. mirabilis, and K. pneumoniae* were clinical isolates fromPig. Albino mice and rats were obtained from the Department of Biochemistry, University of Nigeria Nsukka.

2.2. *Molecular docking*

The 3D structures of fructose-1, 6-bisphosphatase 1, (PDB ID:2JJK) (Mahendran*et.al*, 2014) and human brain AChE in apo form (PDB ID: 3LII) (Dv ir*et al.*, 2010) were used and were retrieved from the Protein Data Bank (PDB), (http://www.pdb.org) database. The structure of the ligand glibenclamide (CID: 91826496). The substrates (inhibitors): N,N'-(heptane-1,7-diyldicarbamoyl)bis(3-chlorobenzenesulfonamide) and N-acetyl-D-glucosamine were separated from 2JJk and 3LII respectively. MMFF94 force field was used for energy minimization of the ligand molecules. Docking calculation was carried out on the protein molecules.

2.3 Synthesis of the ligand, 3-[(E)-(1,5-dimethyl-3-oxo-2-phenyl-2,3-dhydro-1H-Pyrazole-4-yl)diazenyl] pentane-2,4-dione(HDPP)

The preparation followed the method reported by Heinosuke (1967). 4-Aminoantipyrine (0.1884g) was dissolved in dilute HCl and diazotized with $NaNO_2$ at < 5 ^{0}C under stirring. The diazonium salt was poured into a mixture of 6.0 x 10^{-4} moldm^{-3} solution of pentan-2,4-dione and 2.5g/150 cm^3 of CH_3COONa under constant stirring. The product precipitated and was washed with a 1:1 mixture of methanol and water solution. It was recrystallized with methanol and dried over $CaCl_2$ in a desicator (See Scheme 1).

2.4 *Synthesis of the Complexes*

The method reported by El Saied *et al*., (2001) was followed in preparing the complexes. Metal salts were mixed separately with HDPP in 2:1 mole ratio in ethanol. The mixtures were refluxed for 6 h at 60 ^{0}C. The precipitates formed were filtered, washed, and dried over $CaCl_2$ in a desiccator.

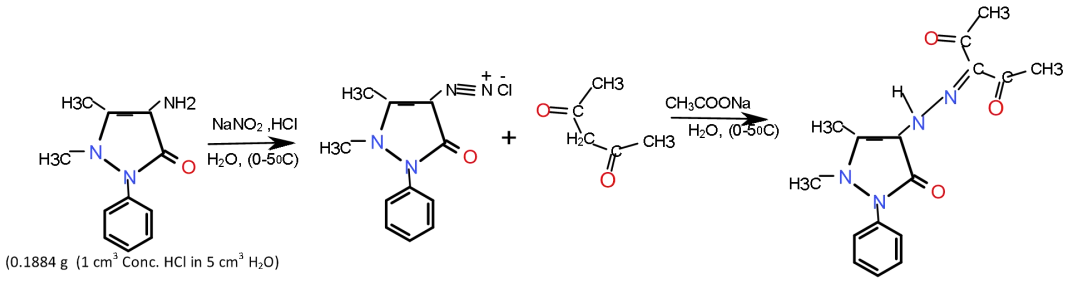

Scheme 1: synthesis of the ligand

3-[1,5-dimethyl-3-oxo-2-phenyl-2, 3-dihydro-1H-pyrazol-4yl) hydrazinylidene]pentane-2,4-dione

2.5 *Antibacterial Screening of HDPP and the complexes*

Preliminary antibacterial screening of the compounds in DMSO was done by Agar – well diffusion method (Mounyr *et al.*, 2016; Heatley, 1944). Already prepared Nutrient agar and Sabouraud Dextrose Agar (SDA) plates were inoculated with 0.1 cm^3 broth culture of the test bacteria. Using a sterile cork borer, wells (5 mm in diameter and 2.5 mm deep) were bored into the inoculated plate. A 50 mg sample of each of the compounds was dissolved in DMSO and equally diluted to yield a concentration between 0.156 to 10 µg/cm^3 for antimicrobial evaluation. Standard antibiotics Ciprofloxacin, Ampicilin and Gentamycin were used as positive control while sterile DMSO served as negative control.

After incubation at 37 ^{0}C, the inhibition zone diameters (IZD) were determined. The

antilog of the intercept on the y-axis of IZD^2 versus the Log (concentration) plot gave the minimum inhibitory concentration (MIC).

2.6 *Acute toxicity(LD_{50}) studies*

All experiments involving the use of mice have been certified to have met the requirements for ethical conduct of research using animals,(Approval Reference Number: FVM-UNN-IACUC-2023-11/132). The Lorke (1983) method was adopted for LD_{50} determination. A total of 144 mice of both sexes were used after acclimatization for 24hours. The mice were placed in three groups of five each and given between 10 to 1000 mg/kg body weight of test compounds separately via 3% v/v normal saline. After 24 h observation, death pattern was noted and used for the second phase where between 1900 and 5000 mg/kg body weight of compounds were offered. A pattern of lethality after 24 h was recorded.

2.7 *Antidiabetic Activities of HDPPand $[Cu(HDPP)_2Cl_2]$*

The method of Owalobi*et al*., (2011) and Osasenaga*et al.,* (2017)were employed for the induction of diabetes in rats using 2% alloxan in saline. Diabetes was confirmed after 72h in rats showing fasting blood sugar level ≥ 200 mg/dl. Diabetic animals were treated with standard drug glibenclamide (5mg/kg body weight) for control and with HDPP and $[Cu(HDPP)_2Cl_2]$ separately. Effects of the compounds as well as glibenclamide on the diabetic rats were determined based on certain parameters (Kottaisamy *et al*., 2021). These include red blood and white blood cell count, Packed cell volume and haemoglobin concentration. Enzymatic antioxidants were assayed based on superoxide dismutase (Guo *et al*., 2022), catalase assay (Ivanović-Matić,*et al*., 2014),glutathione peroxidise (Guo *et al*., 2022) and lipids peroxidation malondaldehyde (Ivanović-Matić,*et al*., 2014). Vitamins C, E and A levels were also determined (Akter *et al.*, 2011).

Serum electrolytes like bicarbonate, chloride, potassium, and selenium were assayed using standard methods (El.Saied *et al.*, 2001). In addition, lipid profiles of the blood samples were determined based on serum cholesterol, serum triglycerides (Mounyr *et al.*, 2016), high-density lipoprotein (Heatley, 1944) and low-density lipoproteins (Lorke, 1983). Kidney function test of diabetic rats was based on the determination (Mounyr *et al.*, 2016) of total protein, creatinine and urea.

2.8 *In silico studies*

Physicochemical properties

The physicochemical properties of HDPP and $[Cu(HDPP)_2Cl_2]$ were generated *in silico*. They include molecular weight (MW), number of hydrogen bond acceptor (HBA), number of hydrogen bond donors (HBD) number of rotatable bonds (NoRB), octanol/water partition coefficient logP(o/w), aqueous solubility (log S) and total polar surface area (TPSA).

2.9 *Drug Target*

Fructose-1,6-biphosphatese(2JJK) and acetycholineesterase (3LII) were the two drug targets studied. Human fructose-1,6-bisphosphatase is a key gluconeogenic enzyme, responsible for the hydrolysis of fructose-1,6-bisphosphate to fructose-6-phosphate. It is a potential drug target in the treatment of type II diabetes. This presents an opportunity for the development of novel therapeutics focused on lowering the hepatic glucose production in type 2 diabetics. Epidemiological studies have provided scientific evidence for a significant association between Type 2 diabetes mellitus (T2DM) and Alzheimer's disease (AD). There are also many clinical and pathological data that suggest a convincing linkage between T2DM and AD (Akter *et al.*, 2011; Park 2011; Priyadarshini *et al*., 2012).Hyperglycemia and insulin dysfunction during diabetes may cause effects on memory, synaptic plasticity and learning which consequently lead to AD (Exalto *et al*., 2012). The association between cholinergic

neurotransmission deficiency and AD provides a base for the development of acetylcholinesterase (AChE) inhibitors as a therapeutic agent (Hitzeman 2006).

3.0 Result and Discussion

3.1 *Single Crystal XRD Data of HDPP*

The single crystal data and structure refinement of HDPP is shown in Table 1 whereas selected bond length and hydrogen bonds are presented in Table 2. The ORTEP diagram and Crystal packing are presented in Figs 1 and 2 respectively. The results showed HDPP to have orthorhombic crystals of Pbca space group and unit cell dimension a = 28.501(4) Å, α = 90°, *b* = 15.0494(19) Å, β = 90°, and *c* = 7.3234(9) Å, γ = 90° for z=8.

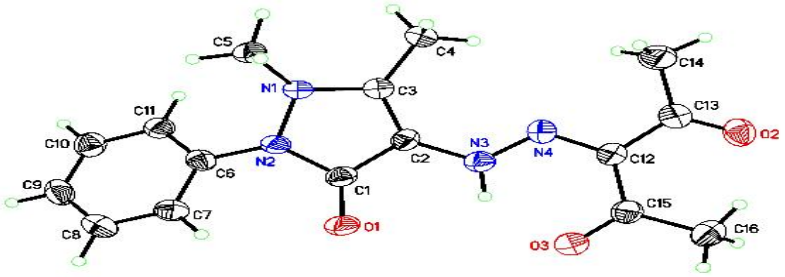

Fig 1.0: The ORTEP diagram of HDPP

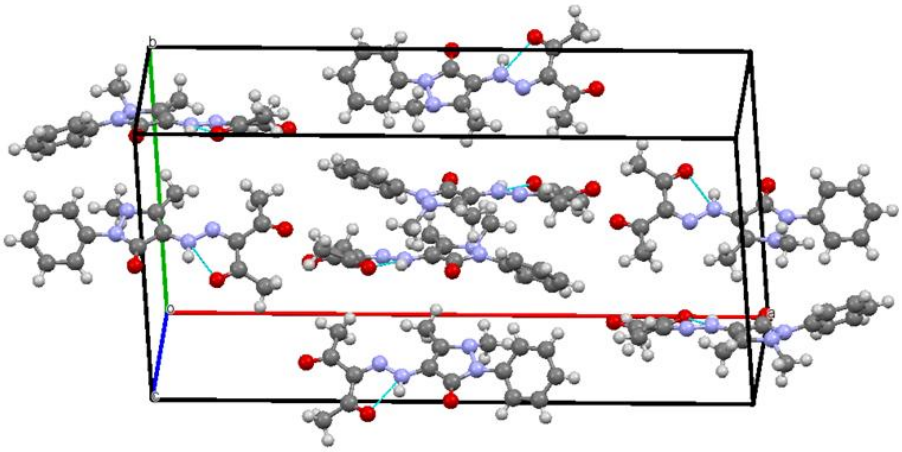

Fig 2.0: Crystal packing of the HDPP

Table 1: Crystal data and structure refinement details of HDPP

Identification code	**HDPP**	
Empirical formula	$C_{16}H_{18}N_4O_3$	
Formula weight	314.34	
Temperature	100(2) K	
Wavelength	0.71073 Å	
Crystal system	Orthorhombic	
Space group	Pbca	
Unit cell dimensions	*a* = 28.501(4) Å	α = 90°
	b = 15.0494(19) Å	β = 90°
	c = 7.3234(9) Å	γ = 90°
Volume	3141.2(7) $Å^3$	
Z	8	
Density (calculated)	1.329 $g.cm^{-3}$	
Absorption coefficient (μ)	0.095 mm^{-1}	
F(000)	1328	
Crystal color, habit	yellow, blocks	

θ range for data collection	2.859 to 27.655°
Index ranges	$-35 \leq h \leq 35, -19 \leq k \leq 19, -8 \leq l \leq 9$
Reflections collected	24321
Independent reflections	3563 [$R_{int} = 0.1288$]
Completeness to θ = 25.242°	99.3 %
Refinement method	Full-matrix least-squares on F^2
Data/restraints / parameters	3563 / 0 / 213
Goodness-of-fit on F^2	1.039
Final R indices [I>2σ(I)]	$R_1 = 0.0604$, $wR_2 = 0.1450$
R indices (all data)	$R_1 = 0.1032$, $wR_2 = 0.1683$
Extinction coefficient	n/a
Largest diff. peak and hole	0.235 and -0.297 $e^{-}.Å^{-3}$

Table 2: Selected Bond lengths [Å] and Bond angles [°]

Atom-atom	distance	atom-atom-atom	Angle
O(1)-C(1)	1.235(3)	C(3)-N(1)-N(2)	106.64(15)
O(3)-C(15)	1.236(3)	N(2)-N(1)-C(5)	114.55(16)
N(1)-N(2)	1.415(2)	C(1)-N(2)-C(6)	125.03(17)
N(2)-C(1)	1.385(3)	N(4)-N(3)-C(2)	122.38(19)
N(3)-N(4)	1.310(2)	C(2)-N(3)-H(3N)	118.8
N(3)-H(3N)	0.8800	O(1)-C(1)-N(2)	126.0(2)
C(1)-C(2)	1.433(3)	N(2)-C(1)-C(2)	104.79(17)
C(3)-C(4)	1.482(3)	C(3)-C(2)-C(1)	109.65(18)
O(2)-C(13)	1.228(3)	C(2)-C(3)-N(1)	108.84(18)
N(1)-C(3)	1.382(3)	N(1)-C(3)-C(4)	120.81(18)
N(1)-C(5)	1.473(3)	C(3)-C(4)-H(4B)	109.5
N(2)-C(6)	1.419(3)	C(3)-C(4)-H(4C)	109.5
N(3)-C(2)	1.393(3)	H(4B)-C(4)-H(4C)	109.5
N(4)-C(12)	1.321(3)	C(3)-N(1)-C(5)	119.00(16)
C(2)-C(3)	1.358(3)	C(1)-N(2)-N(1)	109.51(16)
C(4)-H(4A)	0.9800	N(1)-N(2)-C(6)	121.06(16)
C(4)-H(4C)	0.9800	N(4)-N(3)-H(3N)	118.8
C(5)-H(5B)	0.9800	N(3)-N(4)-C(12)	119.87(19)
C(7)-C(8)	1.383(3)	O(1)-C(1)-C(2)	129.2(2)
C(8)-C(9)	1.375(3)	C(3)-C(2)-N(3)	133.2(2)
C(9)-C(10)	1.381(3)	N(3)-C(2)-C(1)	117.17(19)

****Symmetry transformations used to generate equivalent atoms:**

The X-ray diffractogram recorded 24321 reflections for θ ranging between 2.859 to 27. 650^0 with maxima at θ = 25.242^0. From Table 2, and based on bond lengths, C(1)-O(1), C(13)–O(2) and C(15)–O(3) are double bonds. The slightly higher value of C(15)-O(3) is due to the hydrogen bonding of O(3) to H(3) of N(3). Also N(3) – H(3)….O(3) hydrogen bonding is supported by N(3)- H(3) bond length of 0.8800 Å. N(3) –N(4) bond length of 1.310(2)Å which places in the region of a single bond is further proof of the formation of hydrazone with H-N-N- moiety instead of an azo compound with –N=N- group (Madhavan *et al*., 2012).

3.2 *Physicochemical properties of the compounds*

The yield, melting point, colour, texture, conductivity and qualitative chloride content of synthesized compounds are presented in Table 3.HDPP and its complexes crystallized

in various shades and colour with different textures.

Table 3: Physicochemical properties of HDPP and its complexes

Compound	% Yield	Colour	Texture	M. Pt ^{o}C	Molar. Cond.(Scm^{-1})	Cl^-
HDPP	56.22	Orange yellow	Powdery	138-140	3.8×10^{-7}	Neutral
[Cu(HDPP)$_2$Cl$_2$]	44.72	Black	Granular	74-76	4.5×10^{-6}	Present(IS)
[Ni(HDPP)$_2$Cl$_2$]	58.44	black	Granular	71-72	2.30×10^{-7}	Present(IS)
KCl	-	-	-	-	1.76×10^{-3}	-
CuSO$_4$	-	-	-	--	7.60×10^{-4}	-

Legend *molar conductivity of 0.001 moldm^{-3} solution in methanol, Is= inner-sphere, Os = Outer sphere

This is an indication that new compounds were formed. Melting points of the complexes were sharp and differed much from that of the ligand, also importing the likely formation of new compounds. Conductivities of the complexes when compared to HDPP and controls, $CuSO_4$ (2:2 electrolyte) and KCl (1:1) electrolyte is quite revealing to the values for copper(II) and nickel(II) complexes, as well as HDPP, were lower by between 70 to 10,000 units when compared to the controls. This is an indication that they are non-electrolytes.

3.3. *C, H, N, S. Microanalytical and mass spectral data*

The C, H, N, S. microanalytical and mass spectral data is presented in Table 4. It reveals that the amount of C, N and H calculated theoretically are in close agreement with values determined experimentally and affirm the formulae given to the synthesized compounds as HDPP, [Cu (HDPP)$_2$C1$_2$] and [Ni(HDPP)$_2$ C1$_2$]respectively. HDPP has a molecular formula of $C_{16}H_{18}N_4O_3$ and a molecular mass of 314.345 g/mol. This is in agreement with the molecular ion peak (Fig. 1 in Supplementary materials) of 339.580 which represents $(M+Na)^+$. The absence of $(M-N_2)^+$ peak in the spectrum of HDPP proves that HDPP is a hydrazone and not azo compound (Madhavan *et al*., 2012).

Table 4: The C, H, N, S, Micro analytical data of HDPP and its complexes.

Element	Values	HDPP	[Cu(HDPP)$_2$Cl$_2$]	[Ni(HDPP)$_2$Cl$_2$]
C	Found %	61.55	55.28	50.36
	Cal %	61.15	55.69	50.34
H	Found %	5.44	5.47	5.13
	Cal %	5.73	4.96	4.75
N	Found %	17.77	15.91	14.98
	Cal %	17.83	16.23	14.68

3.4 *Electronic spectral data of the compounds*

The electronic spectra of the HDPP and complexes were recorded in DMSO. These are presented in Fig.s 2- 4 in supplementary materials. HDPP showed maximum absorption at 413.00 nm with molar absorptivity of 265.975 $dm^3mo1^{-1}cm^{-1}$. This absorption is attributed to n-π^*intra-ligand transition. In (Cu(HDPP)$_2$Cl$_2$] and [Ni(HDPP)$_2$C1$_2$] absorbtion band was observed at 427 and 441; 361 and 425 respectively . These bands were assigned to d – d transitions of the metals respectively except that of [Ni(HDPP)$_2$C1$_2$] at 361nm,

which has been assigned to $n \rightarrow \pi^*$ transition. The shift in absorption bands in the complexes is due to complexation which disrupts the electronic structure of the ligand (Holm 1961).

4.5 Infrared spectral data of the compounds

The vibrational frequencies of HDPP and its complexes are shown in Fig. 5-7 in supplementary materials. The broad bands (cm^{-1}) at 3437 in HDPP appeared at 3437 for $[Ni(HDPP)_2C1_2]$ and 3441 for $[Cu(HDPP)_2C1_2]$ and the same is assigned to ν(N-H) stretch (Hassan *et al*., 2020). The shifts prove the involvement of the N-H group in ligation to the metal ions. For the Ni(II) complex, the absence of alteration in the ν (N-H) frequency indicates non-involvement of N-H group in bonding with the ligand. Another point of interest is the carbonyl stretching frequency (ν (C= O) stretch of acetylacetone). It appeared at 1820 cm^{-1} in HDPP but shifted to 1828 cm^{-1}in $[Cu(HDPP)_2C1_2]$. The shifts to higher or lower frequencies indicates involvement of the C=O group in bonding to the metal. The disappearance of this band in $[Ni(HDPP)_2\ C1_2]$ also show involvement of C=O in the formation of this complex. The pyrazolone ring ν(C=O) frequency at1668 cm^{-1} shifted in all the complexes thereby implicating involvement of the pyrazolone C=O in ligation. The ν(C=N) at 1593 cm^{-1} in HDPP remained unchanged in the complex of Cu(II) but shifted in Ni(II) complex underlining involvement of C=N in formation of Ni(II) complex but non-involvement in formation of Cu(II) complex. The strong bands around 1188-1024 cm^{-1} in HDPP and the complexes indicates ν(N-N) stretching modes[2]. The lack of ν (C-O) of eno1 in the spectrum suggests a hydrazone structure for HDPP (Mohahan*et al.*, 2009). The appearance of new bands between 468-531 cm^{-1} underscores the formation of metal-to-ligand bonds of the type M-O and M-N (ElSaied *et al*., 2001), M-C1 bands were not observed (Abdel-Wahab *et al*., 2011; Ajayeoba *et al.*, 2017).

4.6 Nuclear Magnetic Resonance spectra of HDPP and its complexes

The ^1H and ^{13}C NMR spectra of HDPP and the complexes in the $CDC1_3$ solution are shown in Fig. 8-13 in supplementary materials. The signal at 1.8483 ppm (2H, S) shows trace H_2O impurity in the ligand. The proton chemical shift at 2.3704 ppm and 2.52265 ppm (3H,s) are indicative of C-CH_3, N-CH_3 methyl protons of pyrazolone moiety (Mohahan *et al.*, 2009). The other methyl protons have chemical shifts at 3.1409 and 3.4564 ppm for the acetyl groups of the β-diketone. The chemical shift centred between 7.389-7.5359 ppm is due to aromatic protons.

The ^{13}C-NMR spectrum of HDPP (Fig. 13 supplementary materials) shows shifts for 16 carbons on offer. Signals at 129.85, 127.74 and 124.91 ppm represent carbon from two equivalent phenyl ring. Carbon at ortho-position, two at meta-position and one at para-position. The two methyl carbons on the pyrazolone ring have their signals at 11.89 (CH_3-C) and 22.44 ppm (CH_3-N). The two equivalent methyl carbons on the β-diketone moiety gave signal at 36.00 ppm whereas the two equivalent acetyl carbons had shift at 196.04 ppm.The signal at 173.10 ppm is due to the carbonyl group on the pyrazolone ring. The two other carbons of the pyrazolone ring gave signal at 144.57 and 134.66 ppm. Similar assignments had been suggested for such compound in earlier works (Abdel-Wahab et al., 2011). Due to paramagnetic affects, the ^{13}C-NMR spectra of the complexes suffered various degrees of distortions and shifts indicating formation of the complexes.

4.7 Structures of the compounds

Based on all the analytical data provided the following points can be deduced.

(i) HDPP is a hydrazone with a C-NH-N-C group and azo compound.

(ii) HDPP is orthorhombic in its crystalline form and its crystalline form hydrogen bonding occurs.
(iii) HDPP in tridentate and can ligate to metal ions through one acetyl acetyl oxygen, one of or both hydrazinyl nitrogen and through the keto oxygen of the pyrazolone ring.
(iv) The complexes formed are paramagnetic based on various degrees of distortion of their NMR spectra.
(v) Copper(II) complex is octahedral, non-ionic and has the formula $[Cu(HDPP)_2 C1_2]$
(vi) Nickel (II) complex is octahedral, non-ionic and has the formula $[Ni(HDPP)_2 C1_2]$.

On the basis of the accumulated analytical data, the following structures (Fig. 3 – 5) have been proposed for the compounds.

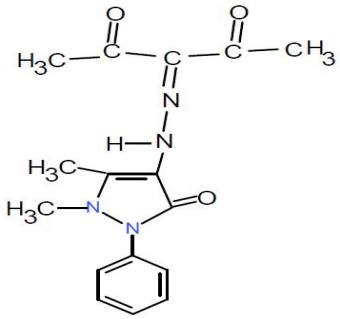

Fig. 3: Structure of HDPP

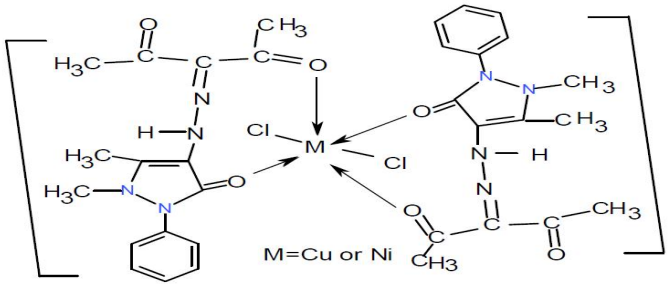

Figs. 4 and 5: Structure of$[Cu(HDPP)_2Cl_2]$ and $[Ni(HDPP)_2Cl_2]$

4.8 Antibacterial Activities

Table 5 shows the zone of inhibition (mm) underlining the sensitivities of the microorganism to the test compounds as well as the controls. HDPP showed no activity against the bacteria strains. However, the complex showed varying degrees of activity against the test organism. Only *S. aureus* was sensitive to $[Ni(HDPD)Cl_2]$. *P. auerignos*a was not sensitive to any of the compounds. The varying degrees of activity could likely be due to the presence of the metal ions which modified the structure of HDPP thereby creating different motifs for binding to bacteria cells (Maheshwari and Shaikh, 2016).

Table 5: Zone of Inhibitions of HDPP and its complexes

Compound	*B.S*	*S.P*	*P.A*	*E.C 6*	*E.C. 13*	*S.A*	*P.M*	*S.I*	*K.P*
HDPP	Nil	Nil	Nil	Nil	Nil	Nil	Nil	Nil	Nil
$[Cu(HDPP)_2Cl_2]$	18	Nil	Nil	Nil	Nil	20	22	22	Nil
$[Ni(HDPP)_2Cl_2]$	0	Nil	Nil	Nil	Nil	15	Nil	Nil	Nil
Ampicilin	0.625	100	100	100	100	2.5	100	2.5	100
Gentamicin	0.1562	2.5	100	100	100	2.5	100	2.5	100
Ciprofloxacin	0.1562	2.5	50	6.25	50	2.5	100	2.5	100

***** B. subtilis = B.S, S.Pneumoniae =S.P, P. aeriginnosa*= P.S.IA, *E. coli(Eco 6) = E.C. 6, E.coli(Eco 13) = E.C. 13, S.aureus = S.A, P.mir abilis = P.M, S.Intermedius (G101)= S.I and K.pneumoniae = K.P***

4.9 Acute toxicity studies

Acute toxicity studies (Table 6) show that for mice administered with HDPP and $[Cu(HDPP)_2Cl_2]$, no animal died at acute dosage implying the safety of these compounds as drug candidates within this range of toxicity category rating dose (Ugwu *et al*., 2018). $[Ni(HDPP)_2Cl_2]$ administered to mice at 1000mg/kg led to some fatalities. Calculated LD_{50} for these compounds was <50mg/kg inferring its high toxicity.

Table 6: Acute Toxicity Studies (LD_{50}) Results of the HDPP and its complexes

Groups	Dosages mg/kg	Mortality HDPP	$[Ni(HDPD)Cl_2]$.	$[Cu(HDPP)_2Cl_2]$	Behavioural changes
		Phase one			
Grp 1	10	0/5	0/5	0/5	Nil
Grp 2	100	0/5	0/5	1/5	Nil
Grp 3	1000	0/5	0/5	1/5	Nil
		Phase two			
Grp 4	1900	0/5	0/5	2/5	Nil
Grp 5	2600	0/5	1/5	3/5	Nil
Grp 6	5000	0/5	1/5	3/5	Weakness ,drowsiness

4.10 In silico studies

The bioavailability of an administered drug in the systemic circulation, which will ultimately determine its ability to bind to the desired receptor to elicit pharmacological activity depends on certain physicochemical parameters. Lipinski has outlined the rule of five (ro5) as a measure of the druggability of a molecule. Thus for a molecule to possess drug-likeness it should have MW ≤ 500, logP ≤ 5, HBD ≤ 5 and HBA ≤ 10. A violation of more than one of these physicochemical parameters disqualifies a compound from being a likely drug candidate(Ugwu *et al*., 2018). Table 7 showed that the ligand and the complex violated none and one of the parameters respectively. Thus they are likely drug candidate. A molecule with the number of rotatable bonds (NoRB) influences bioavailability in rats. NoRB of ≤ 10 has been shown to have good oral bioavailability (Veber *et al*., 2002). These synthesized compounds have NoRB ≤ 10, suggestive of potential good oral bioavailability. Total polar surface area (TPSA) is a measure of cell permeability. A molecule with TPSA of ≤ 140 Å will not have difficulty in permeating the cell membrane. All the compounds fulfilled this requirement. In addition, TPSA of ≤ 90 Å can cross the Blood blood-brain barrier (BBB) and enter the central nervous system (Van de *et al.*, 1998; Ezeokonkwo *et al.*, 2017). This quality is particularly very useful when treating cerebral infections. The ligand has a TPSA of 82.08 Å suggesting its ability to cross the BBB.

4.11 Molecular Docking

The catalytic active site (CAS) of 2JJK was found to interact with glibenclamide through 5 amino acid residues namely: LYS 112, ARG 140, THR 27, LEU 30, GLY 26 (Fig. 8; Table 8). The ligand, which has the highest binding energy (-10.13 kcal/mol) when compared with CuL_2Cl_2 and the co-crystallized inhibitor interacted with the CAS through 7 amino acid residues: THR 27, LEU 30, ARG 140, MET 177, LYS 112, ARG 140, GLY 21 (Fig. 9 – 11). Its activity is comparable to the standard drug. From the foregoing, LYS 112, ARG 140, LEU 30 and THR 27 seem to play vital roles in the activity of 2JJK

Table 7: Physicochemical properties

Compound	MW	HBA	HBD	NoRB	logP(o/w)	LogS	TPSA	LNV
HDPP	314.345	4	1	5	2.701	-2.84	82.08	0
[Cu(HDPP)$_2$Cl$_2$]	775.238	8	4	4	3.088	-4.769	95.22	1

LNV - Lipinski number of violation

Table 8: Free binding energy (ΔG, Kcal/mol) of HDPP and [Cu(HDPP)$_2$Cl$_2$]

Compound	Target	Binding energy, ΔG (kcal/mol)	Interacting amino acid residues
Glibenclamide		-12.01	LYS 112, ARG 140, THR 27, LEU 30, GLY 26
HDPP	2JJK	-10.13	
[Cu(HDPP)$_2$Cl$_2$]		-8.20	THR 27, LEU 30, ARG 140, MET 177, LYS 112, ARG 140, GLY 21
Co-crystallized ligand		-9.39	ARG 22, GLY 28 GLY 26, MET 18, THR 31, GLY 28, GLY 21, LEU 30
Glibenclamide		-9.84	GLU 358, GLY 345, PRO 344
HDPP	3LII	-8.73	PHE 346, GLY 345, SER 347
[Cu(HDPP)$_2$Cl$_2$]		-10.57	4(GLU 358), GLY 345, 2(LEU 353)
Co-crystallized ligand		-9.55	ND

4.12 In vivo anti-diabetic study

Tables 9 - 13 give the results of the assayed parameters as regards the antidiabetic studies. The results of the significant solute in glucose level of diabetic rats treated with HDPP and [Cu(HDPP)$_2$Cl$_2$] and comparable to three treated with glibenclamide, as a standard antibiotic drug at the same dosages are shown below

.

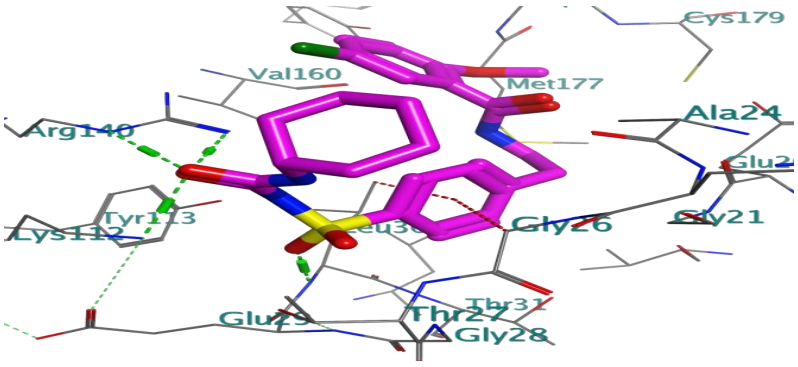

Fig. 8: Interaction of Glibenclamide docked to fructose-1, 6-bisphosphatase 1 (2JJK). The ligand (Glibenclamide) has been shown in 'stick' representation *(green dotted line = H-bond; red dotted line = van der Waal bond)*

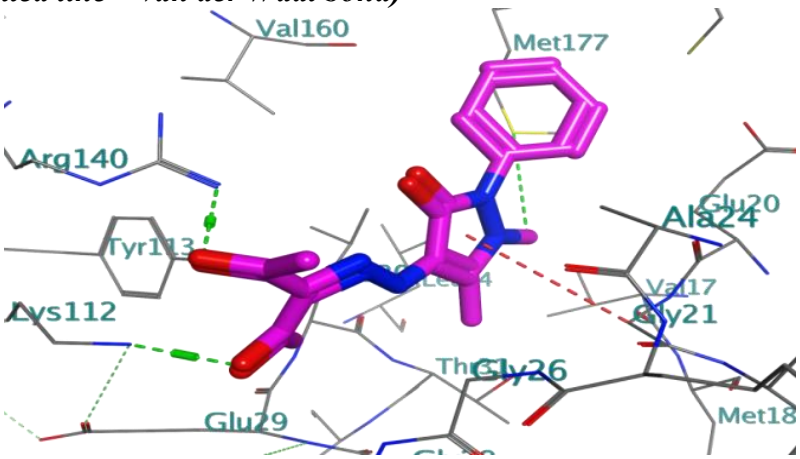

Fig. 9: Interaction of synthesized ligand (HDPP) docked to fructose-1, 6-bisphosphatase 1 (2JJK). The ligand (synthesized ligand) has been shown in the 'stick' representation. *(green dotted line = H-bond; red dotted line = van der Waal bond)*

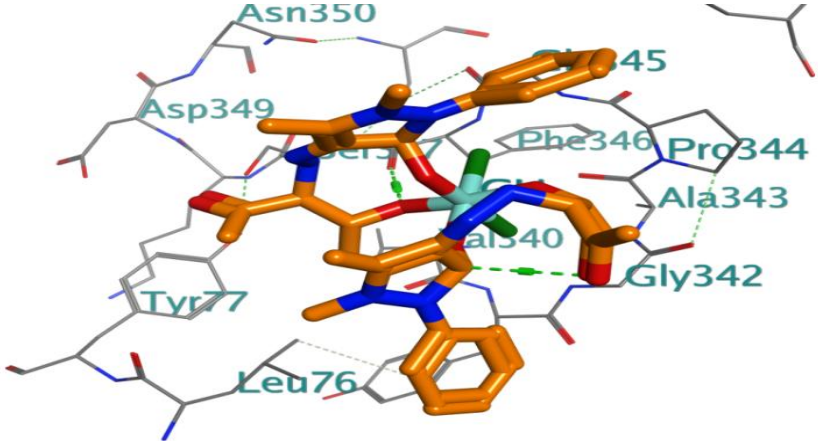

Fig.10: Interaction of synthesized complex [Cu(HDPP)$_2$Cl$_2$] docked to acetylcholinesterase(3LII). The synthesized has been shown in 'stick' representation *(green dotted line = H-bond)*

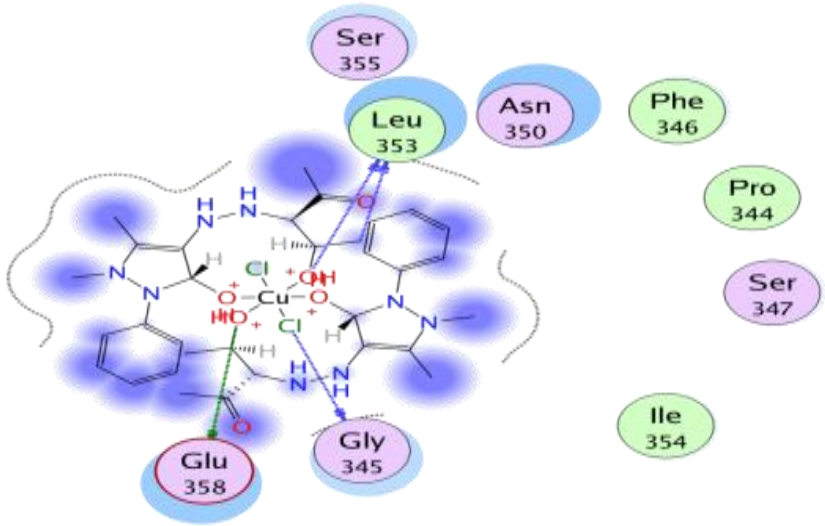

Fig. 11: 2D interaction of synthesized complex $[Cu(HDPP)_2Cl_2]$ docked to acetylcholinesterase (3LII).

Table 9: Effect of the synthesized samples on the blood glucose concentration of alloxan-induced diabetic rats

Groups	Before Induction (mg/dL)	After Induction (mg/dL)	After 7 Days Treatment (mg/dL)	After 14 Days Treatment (mg/dL)	% decrease (7 days)	% decrease (14 days)
A	71.60 ± 6.84^{Abc}	72.40 ± 7.57^{Aa}	74.00 ± 12.85^{Aa}	74.40 ± 7.23^{Aa}		
B	73.40 ± 9.91^{Abc}	308.00 ± 65.36^{Bb}	414.00 ± 45.67^{Cf}	527.80 ± 37.12^{Df}		
C	76.40 ± 5.32^{Ac}	294.60 ± 77.75^{Cb}	175.00 ± 60.38^{Bbcde}	116.20 ± 18.23^{ABabc}	**40.60**	**60.56**
1A	79.80 ± 14.60^{Ac}	321.20 ± 61.76^{Cb}	219.60 ± 85.25^{Bcde}	178.20 ± 60.08^{Bcd}	31.63	44.52
1B	73.40 ± 12.34^{Abc}	317.40 ± 91.05^{Cb}	202.40 ± 71.92^{Bbcde}	124.20 ± 19.55^{ABabc}	36.23	60.87
2A	83.80 ± 5.07^{Ac}	325.40 ± 48.32^{Db}	245.40 ± 39.21^{Cde}	146.40 ± 28.38^{Bbcd}	24.59	55.01
2B	83.80 ± 11.30^{Ac}	349.25 ± 61.68^{Cb}	204.00 ± 62.48^{Bbcde}	117.00 ± 14.97^{Aabc}	41.59	66.50

Results are expressed as mean ± SD (n = 5). Values with different lower case letters as superscripts down the column are significant at $p < 0.05$. Values with different upper case letters as superscripts across the rows are significant at $p < 0.05$.
Group A=Normal Control (No diabetes induction + No treatment)
Group B=Positive Control (diabetes induced + No treatment)
Group C=Standard Control (diabetes induced + treated 200 mg/kg b.w. of Glibenclamide/standard drug)
Group 1A= (diabetes induced + treated with 200 mg/kg b.w. of ligand (HDPP)
Group 1B = (diabetes induced + treated with 400 mg/kg b.w. of ligand (HDPP)
Group 2A= (diabetes induced + treated with 200 mg/kg b.w. of $[Cu(HDPP_2Cl_2]$
Group 2B= (diabetes induced + treated with 400 mg/kg b.w. of $[Cu(HDPP_2Cl_2]$

After seven days of treatment with 200mg/kg body weight of HDPP, diabetic rats having glucose levels of 414.00±45.67mg/100cm^3 were reduced to 219.60 ±85.25 mg/100cm^3. Those treated with 400mg/kg body weight of HDPP had a reduction from 527.80 ±37.12 mg/100 cm^3 to 124.20 mg/ 100cm^3. Rats treated with glibenclamide after 14 days with 100 mg/ kg body weight dosage had glucose level reduction from 527.80 mg/100 cm^3 to 116.20 mg/100 cm^3.

Results obtained using $[Cu(HDPP)_2Cl_2]$ are comparable with percentage reduction at the dosage of 200 mg/kg at 414.00±45.67 mg/100 cm^3 reduced to 245.40±39.21 mg/100 cm^{3}and at 400 mg/kg dosage, 527.80 mg/100 cm^3 reduced to 117.00 mg/100 cm^3 after 14 days treatment.

Table 10: Effect of the synthesized samples on the haematology of alloxan-induced diabetic rats

Groups	WBC (mm^{-3})	RBC (x 10^6 mm^{-3})	PCV (%)	Hb (g/dl)

A	10080±1652.88^{e}	10.72±1.34^{b}	43.00±2.45^{c}	154.71±327.19^{b}
B	4200±678.23^{a}	7.28±0.77^{ab}	35.40±3.58^{a}	11.40±0.97^{a}
C	5880±769.42^{abcd}	10.64±1.22^{ab}	37.80±3.49^{ab}	8.03±0.57^{a}
1A	5440±887.69^{abcd}	10.96±1.46^{ab}	41.60±2.61^{bc}	7.90±0.9 1^{a}
1B	6280±1035.37b^{cd}	10.48±1.25^{ab}	39.80±1.79^{bc}	7.77±0.2 1^{a}
2A	5360±606.63^{abcd}	10.08±1.48^{ab}	41.60±2.97^{bc}	8.01±0.27^{a}
2B	5400±616.44^{abcd}	10.32±1.45^{b}	38.80±2.39^{abc}	7.75±0.3 1^{a}

Table 11: Effect of the synthesized samples on the kidney function test concentration of alloxan induced experimental rats

Groups	Total Protein	Urea	Creatinine
A	5.49±0.45^{e}	23.69±4.40^{ab}	0.49±0.19^{ab}
B	3.61±0.25^{a}	32.50±2.13^{c}	1.60±0.19^{c}
C	5.38±0.32^{de}	24.23±2.25^{b}	0.58±0.26a^{b}
1A	4.74±0.34^{bc}	21.51±3.55^{ab}	0.53±0.20^{ab}
1B	4.85±0.25^{bc}	21.90±2.72^{ab}	0.58±0.13^{ab}
2A	4.70±0.30^{bc}	24.61±1.92^{b}	0.58±0.26^{ab}
2B	4.80±0.40^{bc}	22.05±1.36^{ab}	0.58±0.13^{ab}

Table 12: Effect of the synthesized samples on the liver function test concentration of alloxan-induced experimental rats

Groups	ALT	ALP	AST
A	8.54±0.55^{ab}	27.42±1.85^{ab}	8.28±0.59^{abcd}
B	10.02±0.74^{d}	42.11±2.70^{c}	12.88±0.65^{g}
C	9.43±0.60^{b}	30.47±4.53^{b}	9.15±0.65^{def}
1a	9.26±0.21^{bcd}	29.69±4.53^{ab}	9.21±0.72^{ef}
1b	8.64±0.44^{abc}	30.22±4.12^{ab}	9.32±0.63^{f}
2A	9.17±0.48^{bc}	30.33±3.92^{ab}	9.05±0.71^{cdef}
2B	8.79±0.36^{abc}	30.72±4.10^{b}	8.85±0.27^{bcdef}

Table 13: Effect of the synthesized samples on the Antioxidant Concentration on Alloxan Induced Experimental Rats

Groups	GSH	SOD	GPx	CAT	MDA
A	2.49±0.28^{abcd}	11.09±0.18^{ab}	12.76±1.12b	1.14±0.06a^{b}	1.49±0.28^{c}
B	3.41±0.52^{e}	11.46±0.01^{d}	12.76±2.06^{b}	2.38±0.47^{f}	2.24±0.34^{d}
C	2.58±0.24^{abcd}	11.24±0.21^{abcd}	10.51±1.42^{a}	1.25±0.04^{abcd}	1.29±0.21^{abc}
1A	2.59±0.17^{abcd}	11.36±0.06^{cd}	11.38±1.42^{ab}	1.35±0.13^{cde}	1.39±0.17^{bc}
1B	2.71±0.06^{d}	11.32±0.07^{bcd}	11.03±1.66^{a}	1.44±0.11^{de}	1.43±0.32^{bc}
2A	2.74±0.08^{d}	11.32±0.18^{bcd}	11.21±1.06^{ab}	1.46±0.09^{e}	1.34±0.11^{abc}

2B	2.68±0.10^{cd}	11.37±0.70^{cd}	11.03±1.13^{a}	1.40±0.12^{de}	1.26±0.06^{abc}

(HDPP) In all, results are expressed as mean ± SD (n = 5). Values with different lowercase letters as superscripts down the column are significant at p < 0.05. Values with different upper case letters as superscripts across the rows are significant at p < 0.05.
Group A=Normal Control (No diabetes induction + No treatment)
Group B=Positive Control (diabetes induced + No treatment)
Group C=Standard Control (diabetes induced + treated 200 mg/kg b.w. of Glibenclamide/standard drug)
Group 1A= (diabetes induced + treated with 200 mg/kg b.w. of ligand (HDPP)
Group 1B = (diabetes induced + treated with 400 mg/kg b.w. of ligand
Group 2A= (diabetes induced + treated with 200 mg/kg b.w. of [Cu(HDPP$_2$Cl$_2$]
Group 2B= (diabetes induced + treated with 400 mg/kg b.w. of [Cu(HDPP$_2$Cl$_2$]

Other blood parameters analysed showed positive levels after treatment with HDPP and [Cu(HDPP)$_2$Cl$_2$]. Liver and kidney functions of the diabatic rates were better on treatment with the ligand and its Cu(II) complex. The compounds showed good antioxidant activities.

4.0 Conclusion

For the first time the ligand, HDPP has been synthesized and completely characterized via single crystal XRD proving its hydrazone form and not azo form as suggested by some earlier workers. Also, for the first time, its antidiabetic potentials were assayed. This compound has great potential as an antidiabetic drug as well as its Cu(II) complex.
HDPP and its Cu (II)and Ni(II) complexes were also synthesized. Biological studies indicated HDPP and [Cu(HDPP)$_2$Cl$_2$] to be non-toxic and therefore were assigned for antidiabetic screening. *In silico* studies proved favourable drug-likeness properties for HDPP and [Cu(HDPP)$_2$Cl$_2$] and molecular docking unto drug targets 2JJK and 3LII as well as with fructose,-1,6-biphosphate, a key glucogenic enzyme indicated the amino acid side chains responsible for drug action. *In vivo* antidiabetic studies via induction with alloxan induced rats revealed closeness of activity of HDPP and [Cu(HDPP)Cl$_2$] with glibenclamide (diabetes control drug).

Acknowledgement

Ukoha, P.O. thanks the Department of Pure and Industrial Chemistry, University of Nigeria Nsukka for providing bench space and technical assistance.

5.0 References

Abdel-Wahab, B.F., Awad, G. E., & Badria, F. A .(2011). Synthesis, antimicrobial, antioxidant, anti-hemolytic and cytotoxic evaluation of new imidazole-based heterocycles”., *Eur. J. Med.Chem*., 46, pp. 1505 – 1511.

Ajayeoba, T, A., Akinyele, O. F., & Oluwole, A. O. (2017).Synthesis, characterisation and antimicrobial studies of nixed Nickel(II) and Copper(II) complexes of Aroylhydrazones with 2,2^1-bipyridine and 1,10-phenanthroline. *Ife Journal of Science*, 19, 1, pp. 119-132. https://dx.doi.org/10.4314/ijs.v19i1.12

Akter, K., Lanza, E. A., Martin, S. A., Myronyuk, N., Rua, M., & Raffa, R. B. (2011). Diabetes mellitus and Alzheimer’s disease: shared pathology and treatment. *Br J Clin Pharmacol.,* 71, pp. 365–376.

Blonde, L. (2005). Current challenges in diabetes management; *Clin.Cornerstone,* 7, 3, pp. S6-S17. DOI: 10.1016/s1098-3597(05)80084-5

Budesinsky, B. & Svecova, A. (1970). A new metallochromic reagent:

Photometric Determination of Cobalt and Scandium. *J.Anal.Chim.Acta*, 49, 2, pp. 231- 240.

Dvir, H., Silman, I., Harel, M., Rosenberry, T. L., & Sussman, J. L. (2010). Acetylcholinesteras:From 3D structure to function. *Chem.Biol.Interact* 187, pp. 10-22.

El.Saied, F. A., Ayad, M. I., Issa, R. M., & Aly, S. A. (2001). Synthesis and charactersation of Iron(III),Cobalt (II),Nickel(II) and copper(II) Complexes of 4-formylazohydrazoaniline Antipyrine, *Polish. J .Chem.,*75, 6, pp. 773 – 783.

Exalto, L., Whitmer, R., Kappele, L., & Biessels, G. (2012) An update on type 2 diabetes, vascular dementia and Alzheimer's disease. *Exp Gerontol* 47,pp. 858–864.

Ezeokonkwo, M. A., Ogbonna, O. N., Okafor, S. N., Godwin-Nwakwasi, E. U., Ibeanu, F. N., & Okoro, U. C. (2017). Angular Phenozaxine Ethers as Potent Multi-microbial Targets Inhibitors: Design, Synthesis, and Molecular Docking Studies. *Front. Chem.* 5:107. https://doi.org/10.3389/fchem.2017.00107

Ghaib, A., Ménager, S., Vérité, P., & Lafont, O.(2002). Synthesis of variously 9,9-dialkylated octahydropyrimido [3,4-a]-s-triazines with potential antifungal activity. *IL Farmaco,*57, 89, pp. 109 – 116.

Guo, J., Liu, H., Zhao, D., Pan, C., Jin, X., Hu, Y., Gao, X.,. Rao, P. & Liu. (2022). "Glucose-lowering effects of orally administered superoxide dismutase in type 2 diabetic model rats". *npj Sci Food,* 6, 36, doi: 10.1038/s41538-022-00151-5

Hassan, F., Fayez, M.& Abdalla, S. J. (2020). Synthesis, characterization, anti -bacterial, and antifungal activities of cobalt(II), nickel(II) and copper(II) complexes with 3-thioacetyl-2-amino-1,4-naphthoquinone and 2-benzoyl-3-amino-1,4-naphthoquinone Ligands. *Open Journal of Inorganic Non-metallic Materials*, 10, pp. 45-61. doi: 10.4236/ojinm.2020.104004.

Heatley, N. G. (1944). A method for the assay of penicillin, *Biochem J*, 38 (1), pp. 61–65. doi: 10.1042/bj0380061.

Heinosuke, Y.(1967). Infrared Analysis of 2-pyrazolin-5-one Derivatives, *Applied Spectroscopy,* 23(1), 1969. pp. 22 – 28.

Hitzeman, N. (2006) Cholinesterase inhibitors for Alzheimer's disease. *Am Fam Physician* 74, pp. 747–759.

Holm, R. H. (1961). *Spectral and magnetic studies of substituted nickel(II) salicylaldimine complexes. In advances in the chemistry of coordination compounds*; Kirschner, S., Ed.; MacMillan: New York, pp. 341-349.

Issa, R. M., Abdel-Latif, S. A., & Abdel-Salam, H. A. (2001). *Synth. React. Inorg. Met.-Org.Chem.,*31, 95-105. DOI. 10.1081/SIM-100001935

Ivanović-Matić, S., Bogojevic, D., Martnivic, V., Petrovic, A., Jovanovic-Stojanov, S., Poznanovic, G. & Grigorov, I. (2011). "Catalase inhibition in diabetic rats potentiates DNA damage and apoptotic cell death setting the stage for cardiomyopathy". *J. Physiol Biochem.*, 70, 4, pp. 947-959.

Kottaisamy, C.P.D., Raj, D.S., Prasanth Kumar, V., Sankaran, U.(2021) Experimental animal models for diabetes and its related complications—a review. *Lab Anim Res* **37**, 23. https://doi.org/10.1186/s42826-021-00101-

Lorke, D. (1983). A new approach to practical acute toxicity testing. *Archaeology of Toxicology*, 54, pp. 275-287.

Madhavan, S. N., Dasan, A., &Raphael, S. J. (2012). Synthesis, characterization, antifungal, antibacterial and DNA cleavage studies of some heterocyclic Schiff base metal complexes".*Journal of Saudi Chemical Society,* 16, 1, pp. 83-88.

Mahendran, G., Manickam, M., Murugesh, E., Kumar, R. S., Shanmughavel, P., Prasad, K. J, R.&Bai, V. N.(2014). ¨*In vivo* anti-diabetic, antioxidant and molecular docking studies of 1, 2, 8-trihydroxy-6-methoxy xanthone and 1, 2-dihydroxy-6-methoxyxanthone-8-O-β-D-xylopyranosyl isolated from *swetia corymbosa*" . *Phytomedicine,* 21, 11, pp. 1237-1248.

Maheshwari, D. G.& Shaikh, N.K. (2016). An overview on toxicity testing method". *Int. J. Pharm. Technol.* 8, 2, pp. 3834-3849.

Mohahan, K., Athira, C. J., Sindhu, Y.& Sujamol, M. S. (2009).Synthesis, spectroscopic characterization and thermal studies of some lanthanide(III) nitrate complexes with a hydrazo derivative of 4-aminoantipyrine. *Journal of rare earths*, 27, 5, pp. 705-710.

Morgan, G.T & Reilly, J.(1913) Synthesis of a red azo compound(Azonol A) from pentan-2,4-dione and 4-aminoantipyrine. Journal of Chemical Society, 103, pp. 808, 808.

Mounyr, B., Moulay, S.& Saad, K. I. (2016). Methods for in vitro evaluating antimicrobial activity: A review. *Journal of Pharmaceutical Analysis*" 6, 2, pp. 71-79.

Nawar, N. & Hosny, N. M. (2000). Synthesis, spectral and antimicrobial activity studies of o-aminoacetophenone o-hydroxybenzoylhydrazone omplexes. *Transition Met. Chem.,*25, pp. 1- 8.

Osasenaga, M. I., Abiola, M. A. & Oluseyi, A. A. (2017). Alloxan-induced diabetes, a common model for evaluating the glycemic-control potential of therapeutic compounds and plants extracts in experimental studies" *Medicina (Kaunas)*; 53, 6, pp. 365-374.

Owolabi, O.J., Amaechina, F.C., & Okoro , M. (2011). Effect of ethanol leaf extract of newbouldia laevis on blood glucose level of diabetic rats. *Tropical Journal of Pharmaceutical Research,* 10, pp. 249-254.

Ozmen, U¨ O. & Olgun, G. (2008). Synthesis, Characterization and antibacterial activity of new sulfonyl derivatives and their Ni(II) Complexes. *Spectrochimica Acta Part A*, 70, pp. 641–645.

Park, S. (2011). A common pathogenic mechanism linking type-2 diabetes and Alzheimer's disease evidence from animal models. *J Clin Neurol* , 7, pp. 10–18.

Priyadarshin,i M., Kamal, M. A., Greig, N. H., Realef, M., Abuzenadah, A. M., Chaudhary, A. G. A.& Damanhouri, G. A. (2012) Alzheimer's disease and type 2 diabetes: exploring the association to obesity and tyrosine hydroxylase.*CNS and Neurological Disorders- Drug Targets*, 11, pp. 482–489.

Rao, S., Mishra, D.D., Mourya, R. V. & Nageswara, N.(1997). Oxovanadium binuclear (IV) Schiff base complexes derived from aroyl hydrazones having a subnormal magnetic moment. *Polyhedron* 16, pp. 1825- 1829.

Ravindran, R. (2004). Synthesis and characterisation of iron(III) complexes of 1,2-dihydro-1-phenyl-2,3-dimethyl-4-[2¢,4¢-pentanedione-3¢hydrazono -]pyrazol-5-one**,** *Indian Journal of Chemistry*, 43A, pp. 1245-1248.

Rollas, S. & Küçükgüzel, Ş. G. (2007). Biological activities of Hydrazone derivatives.*Molecules,* 12, pp. 1910-1939.

Sari, N., Nartop, D., Karci, F. & Disli, A. (2008). Novel Hydrazone Derivatives and Their Tetracoordinated Metal Complexes. *Asian Journal of Chemistry,* 20, 3, pp. 1975-1985.

Sarwar, N., Gao, P., Kondapally Seshasai, S. R., Gobin, R., Kaptoge, S., Di Angelantonio, E., Ingelsson, E., Lawlor, D. A., Selvin, E., Stampfer, M., Stehouwer,C. D. A., Lewington, S., Pennells, L., Thompson, A., Sattar, N., White, I. R., Ray, K. K., &Danesh, J. (2010). Diabetes mellitus, fasting blood

glucose concentration, and risk of vascular disease: a collaborative meta-analysis of 102 prospective studies. *Lancet* 375, 9733, pp. 2215-2222.

Sivasankar, B. N. & Gavindaragam, S. (1995). *Synth. React. Inorg. Met.-Org. Chem.*, 25, pp.127 – 131.

Ugwu, D.I., Okoro, U.C., Ukoha, P.O., Gupta, A. & Okafor, S.N. (2018). Novel anti-inflammatory and analgesic agents: synthesis, molecular docking and in vivo studies. *Journal of Enzyme Inhibition and Medicinal Chemistry*. 33, 1, pp. 405–415.

Van de, W. H., Camenish, G., Folkers, G., Chretien, J. R. & Raevsky, O.A. (1998). Estimation of blood-brain barrier crossing of drugs using molecular size and shape, and H-bonding characteristics. *J. Drug Target* 6, pp. 151–165.

Veber, D. F., Johnson, S. R., Cheng, H. Y., Smith, B. R., Ward, K. W., Koppel, K. D.(2002). Molecular properties that influence the oral bioavailability of drug candidates. *J Med Chem*. 45, 12, pp. 2615–2623.

Zdzislaw, B., Jaroslaw, S., Anna, K., Ewa, K., Maria, G. (2009). Heterocyclic Chem. 46, 6, pp. 1396-1403.

Compliance with Ethical Standards Declaration

Ethical Approval

Not Applicable

Competing interests

The authors declare that they have no known competing financial interests

Funding

The authors declared no external source of funding.

Availability of data and materials

Data would be made available on request.

Author Contributions

Conceptualization and methodology: Pius Onyeoziri Ukoha, Ndidiamaka Justina Agbo, Uchechukwu Susan Oruma.

Software: Oguejiofo T. Ujam, Tania Groutso, Okereke Solomon Ejike.

Validation, Oguejiofo T. Ujam, Tania Groutso.

Formal analysis: Ndidiamaka Justina Agbo, Uchechukwu Susan Oruma.

Resources: Pius Onyeoziri Ukoha, Ndidiamaka Justina Agbo, Uchechukwu Susan Oruma, Okereke Solomon Ejike.

Writing—original draft preparation: Pius Onyeoziri Ukoha, Ndidiamaka Justina Agbo, Uchechukwu Susan Oruma.

Writing—review and editing: Pius Onyeoziri Ukoha, Ndidiamaka Justina Agbo, Uchechukwu Susan Oruma, Oguejiofo T. Ujam, Okereke Solomon Ejike

Supervision: Pius Onyeoziri Ukoha.

All authors have read and agreed to the published version of the manuscript.